a reprint from Applied Optics

Derivation of Mount Pinatubo stratospheric aerosol mean size distribution by means of a multiwavelength lidar

Massimo Del Guasta, Marco Morandi, L. Stefanutti, B. Stein, and J. P. Wolf

A multiwavelength lidar operated in Sodankyla, Finland, during the European Arctic Stratospheric Ozone Experiment (December 1991–March 1992). It produced vertical profiles of stratospheric aerosols at four wavelengths. The determination of aerosol mean size distribution has been performed by use of extinction/backscattering ratios as obtained from lidar data processing at 355, 352, and 750 nm. Log-normal distributions of sulfuric particles with mode radius of r_m = 0.12–0.25 μm and corresponding widths of s = 2–1.6 have been retrieved as best fits of experimental data, in good agreement with *in situ* measurements. A successful attempt to derive bimodal log-normal distributions is also described, together with the experimental and theoretical problems involved.

Key words: lidar, Mie scattering, aerosol sizing.

1. Introduction

Volcanic eruptions represent a natural episodic source of stratospheric aerosols capable of increasing by several magnitudes the background aerosol concentration, as occurred recently after the eruption of Mt. Pinatubo in the Philippines (in June 1991). As a consequence perturbations in the stratospheric chemistry processes can occur.

The stratospheric aerosol particles are expected to be composed of concentrated sulfuric acid, and their size assumes a primary role in the heterogeneous reactions involved in ozone chemistry.

In this paper lidar measurements at four wavelengths have been used to retrieve single and bimodal mean size distributions of Mt. Pinatubo's stratospheric layer, starting from a large set of such measurements collected during the European Arctic Stratospheric Ozone Experiment (EASOE) campaign in Sodankyla, Finland (66° N) from December 1991 to March 1992.

M. Del Guasta, M. Morandi, and L. Stefanutti are with the Istituto di Ricerca Sulle Onde Elettromagnetiche, Consiglio Nazionale delle Ricerche, Florence, Italy. B. Stein and J. P. Wolf are with the Freie Universität, Arnimallee 14 Berlin, Germany D-14195.

Received 2 June 1993; revised manuscript received 3 January 1994.

0003-6935/94/245690-08$06.00/0.

2. Experimental Setup

The main characteristics of the lidar system, described by Stefanutti *et al.*,[1] are as follows.

Two lasers are used as transmitters: (a) a Nd–YAG laser supplied with both second- and third-harmonic generators, with a 10-pps repetition rate, 0.5-mr full-angle divergency, and pulse energies of 400 mJ at 532 nm and 120 mJ at 355 nm and (b) a tunable Ti–sapphire laser with a 10-pps repetition rate and 2-mr full-angle divergency and pulse energies of 300 mJ at both 750 and 850 nm (750- and 850-nm emissions have been used in the EASOE campaign).

A 0.5-m-diameter telescope, with a 0.6-mr (full-angle) field of view and two crossed polarization detection channels, is used as a receiver. Photomultipliers with S20 cathodes were used as detectors.

The acquistion system (LeCroy Corp.) is based on two 12-bit 5-MHz waveform recorders (permitting a vertical resolution of 30 m) and a personal computer for data storage.

Three rawinsonde soundings a day and three ozone electrochemical soundings a week were carried out by the Finnish Meteorological Institute.

The four-wavelength lidar operated in Sodankyla, Finland, from 2 December 1991 to 12 March 1992. Multiwavelength measurements have been performed, all on clear-sky days, by integrating over 1000–5000 laser shots for each wavelength. In Fig. 1 a complete multiwavelength measurement is shown in terms of squared-range-corrected lidar signals.

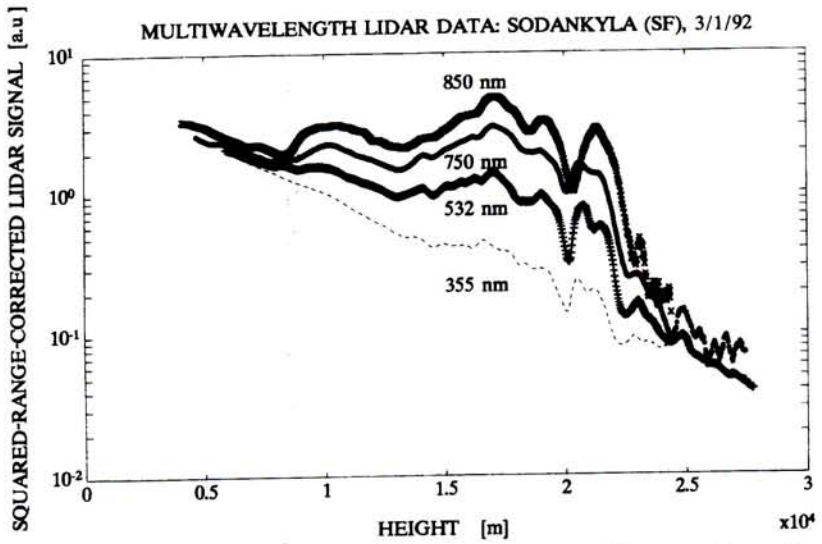

Fig. 1. Sample of multiwavelength lidar measurement. The squared-range-corrected lidar signals are shown in arbitrary units. The three profiles are almost simultaneous, the downward slope being given by the molecular scattering. By processing such profiles, aerosol backscattering and extinction/backscattering ratios are obtained.

3. Lidar Data Inversion

Several inversion algorithms, such as those suggested by Klett[2,3] and a simple iterative numerical solution developed by Morandi,[4] have been tested. The results of these tests have also been compared with results obtained by the use of a different method developed by Kolenda *et al.*[5]

A simulation program was written to evaluate the errors and to compare the accuracy of the different procedures. Such a program simulates a Rayleigh atmosphere to which aerosol profiles can be added and generates a lidar return, including a statistical noise. The optical parameters can be retrieved by means of different routines; tests performed by Morandi[4] show that the errors in retrieved optical quantities do not significantly depend on the method used for the data processing. This is also true in spite of substantial differences between the methods, such as different modeling of the dependence between extinction and backscattering coefficients. Critical sources of error are the uncertainties on the molecular density profile and the *a priori* hypothesis about the actual value of the scattering ratio at the cloud base.

The program used for the data processing works as follows. The rawinsonde data file closest to the lidar acquisition is automatically searched, and the five coefficients of the density fitting function,

$$d(z) = \exp(c_1 + c_2 z + c_3 z^2 + c_4 z^3 + c_5 z^4), \qquad (1)$$

are computed on the basis of the measured density profiles.

The squared-range-corrected lidar return is converted into a backscattering profile by fitting the signal to the molecular profile obtained with Eq. (1). The fitting range is chosen to be above the cloud top, in a region in which the signal behavior denotes an aerosol-free atmosphere.

The scattering ratio defined by

$$R = (\beta_a + \beta_m)/\beta_m,$$

with β_m = molecular backscattering and β_a = aerosol backscattering, is assumed to be 1 at the cloud top, so that the value $\sigma_R(z_m)$ of the molecular extinction coefficient can be used as the reference value σ_m at the upper edge z_m of the integration interval of the Klett[2] method. The dependence between the extinction $[\sigma(z)]$ and the backscattering $[\beta(z)]$ coefficients is assumed to be of the form

$$\beta(z) = K_1 \sigma(z)^{K_2}, \qquad (2)$$

as suggested by several papers on atmospheric aerosols, for example, Ref. 6. The standard backward Klett's method, involving only a bound (σ_m), is not capable of giving a value for K_2. The dependence of $\beta(z)$ on $\sigma(z)$ can be reduced to a linear law by putting $K_2 = 1$; otherwise a value of K_2 can be computed by imposing a second bound, below the aerosol layer; this second approach has been used in our analysis. An arbitrary value of the scattering ratio below the Mt. Pinatubo cloud, around the tropopause, has been imposed. We call Ro_j such an arbitrary value, where the subscript j indicates the wavelength. Under the hypothesis that $R = Ro_j$ and $R = 1$ at the aerosol layer base and top, respectively, and starting from an arbitrary value of K_2, we show that the inversion routine is iterated, the value of K_2 being varied step by step, until a good fit between the molecular profile and the extinction-corrected lidar return is achieved.

The aerosol size distribution has been estimated by investigating the dependence on the wavelength of the extinction/backscattering ratio. For each extinction-corrected lidar return at wavelength j, a mean aerosol extinction/backscattering coefficient k_j has been computed as the ratio between the aerosol

optical depth and the integrated aerosol backscattering ratio. Aerosol optical depth and integrated aerosol backscattering have been obtained after the subtraction of molecular extinction and backscattering profiles from the corrected lidar profiles.

The high sensitivity of k_j to the arbitrary hypothesis on Ro_j represents the most critical problem in such an approach. Tests have been performed both on real 532-nm lidar profiles acquired in Sodankyla and on simulated aerosol layers with a similar optical depth. Results show that a change of approximately +5% in Ro_j produces a variation of approximately −20% in retrieved k_{532}.

All the profiles showing the presence of cirrus clouds have been rejected in our data analysis so as to avoid large errors in k_j because of either wrong values of Ro_j or substantial differences in the aerosol particle shape and size between the cirrus and the Mt. Pinatubo layers. For the 532-nm wavelength Ro was assumed to be in the range 1–1.05, which should cover most of the possible conditions at the polar Mt. Pinatubo cloud's base. The scattering ratio Ro depends on the wavelength of the lidar. If a maximum of 1.05 could represent a reasonable upper limit of Ro_j for both 355- and 532-nm wavelengths, higher values are expected for longer wavelengths, and quite large k_j relative errors must be expected for the two near-IR wavelengths, 750 and 850 nm.

For fixed values of Ro_{532} (Ro_{532} = 1, 1.03, 1.05, 1.07, 1.1) we computed Ro_j at the other three wavelengths, according to the wavelength scaling of the backscattering in the lowest part of the Mt. Pinatubo cloud. Starting from the raw backscattering profiles, we iterated the procedure several times. Each iteration that the extinction profile retrieved by the use of the previous value of Ro_j was used to correct the raw lidar return, then a new Ro_j was computed from the new backscattering scaling. After a few iterations the scaling factors converged to stable values. This way only Ro_{532} persists as an arbitrary parameter.

For each value of Ro_{532} the lidar data inversion provided a large set of k_j for all four wavelengths. Both the k_{532} and the k_{355} parameters show a smaller statistical dispersion than the k_{750} and the k_{850} parameters. As a consequence, the 532- and the 355-nm data play a preponderant role in the least-square method used to compute a monomodal log-normal size distribution. When a bimodal size distribution is considered, all the wavelengths contribute to define the least-square minimum, and statistical errors grow much larger.

4. Scattering Simulations

Simulations of the scattering properties of spherical aerosols were performed with van de Hulst[7] results in a computer program developed by Del Guasta.[8] A data set of backscattering and extinction efficiencies as functions of the size parameter (α) was produced for values of the refractive index corresponding to those of ice, water, and several concentrations of sulfuric acid solutions (25%, 30%, 50%, and 75%). The refractive indices of sulfuric acid, at the various wavelengths and for different concentrations, were obtained from the data of Palmer and Williams,[9] whereas for ice we used the data reported by Warren.[10] The imaginary part of the refractive index has been neglected for both the 532- and the 355-nm wavelengths. The correction of refractive indices (generally measured at room temperature) for stratospheric temperatures has also been neglected.

Simulations have been performed for the four lidar wavelengths and for the size parameter α, ranging from 0 up to 100 in steps of 0.01. The simulation program computes the backscattering and the extinction cross sections and their ratio k_j by integrating the scattering efficiences over the selected size distributions.

Both monomodal and bimodal log-normal distributions have been used to model the stratospheric aerosols, as suggested by studies such as those of Hofmann *et al.*[11] and Brogniez and Noble.[12]

The monomodal log-normal distribution here is given by

$$N(r) = \frac{Nt}{\sqrt{2\pi} r \ln(s)} \exp\{-0.5[\ln(r/r_m)/\ln(s)]^2\}, \quad (3)$$

with r_m = mode radius, s = width, and Nt = total aerosol number.

Scattering simulations for monomodal distributions have been performed with variable r_m and s, a database of β_j, σ_j, and k_j for a single particle (Nt = 1) having been produced by varying the two parameters with steps of 0.02 μm for r_m and with steps of 0.02 for s. r_m and s have been varied between 0 and 2 μm and between 1.1 and 2, respectively, ranges expected for stratospheric volcanic aerosols.

Archive files containing such simulations have been produced for ice, water, and several sulfuric acid solutions in the range 25–75%.

5. Size Distribution Retrieval Method

The processing of each multiwavelength lidar measurement gives us several optical quantities, such as $\{\beta_j\}$, $\{\sigma_j\}$, and $\{k_j\}$.

To assess which of these quantities are the most promising for size distribution retrieval, a test was performed on simulated $\{\beta_j\}$, $\{\sigma_j\}$, and $\{k_j\}$, computed as described in Section 4 for monomodal distributions. It is possible to check the sensitivity of $\{\beta_j\}$, $\{\sigma_j\}$, and $\{k_j\}$ with respect to the size distribution parameters r_m and s. To do this, we have plotted $\{\beta_j\}$, $\{\sigma_j\}$, and $\{k_j\}$ by the use of constant-value plots (e.g., Fig. 2, below) as functions of r_m and s. In such plots, each aerosol size distribution is characterized by a pair (r_m, s) corresponding to a point on the plot. For each point (r_m, s) four constant-level lines of $\{\beta_j\}$, $\{\sigma_j\}$, or $\{k_j\}$ (corresponding to the four wavelengths j) are crossing. The most sensitive quantity $\{q_j\}$ among $\{\beta_j\}$, $\{\sigma_j\}$, and $\{k_j\}$ is the one whose four constant-value lines form the widest crossing angles; in such a condition a slight change in r_m or s produces a major change in the four

q_j, a change that is detectable by lidar. According to our analysis, $\{k_j\}$ turned out to be the most promising quantity, being strongly sensitive to changes in r_m and s. Figures 2–5 show plots of computed k_{532} and k_{750} for monomodal distributions of sulfuric aerosols.

The fundamental advantage in considering k_j for size retrieval is that it does not depend on the aerosol number density in the single-scattering approximation. Mean values of k_j, therefore, can be computed by averaging values retrieved from many lidar profiles, regardless of temporal changes in the cloud's profile (at least when no dramatic changes in the aerosol size distribution are expected).

The histograms shown in Figs. 6–9 show the occurrence of experimental k_j values in EASOE data; such values are obtained by the use of $Ro_j = 1$ for all wavelengths. Figure 10 shows the dependency of k_j on Ro_{532} for all four wavelengths.

The experimental mean values of k_j with the associated sample standard deviations σ_j are listed in Table 1 for the hypothesis that $1 < Ro_{532} < 1.05$. These mean values of k_j and σ_j have been obtained by Morandi[13] by processing the whole EASOE multiwavelength lidar data set.

Searching for a size distribution, we performed a comparison between simulated and experimental k_j's, the least-square method having been used to search for the minima of the χ^2 function:

$$\chi^2(r_m, s) = \sum_{j=1}^{3} [(k_j - k_{sj})/\sigma_j]^2, \qquad (4)$$

where σ_j is the standard deviation of the experimental k_j data at wavelength j and k_{sj} is the theoretical value

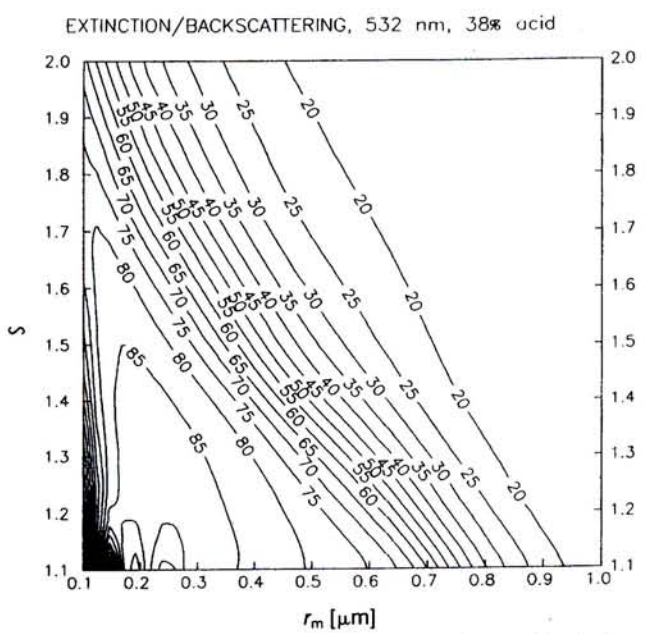

Fig. 2. Extinction/backscattering ratio at 532 nm (k_{532}) simulated for monomodal log-normal distributions of 38% sulfuric acid droplets. The x axis is the mode radius r_m, and the y axis is the distribution dimensionless width s.

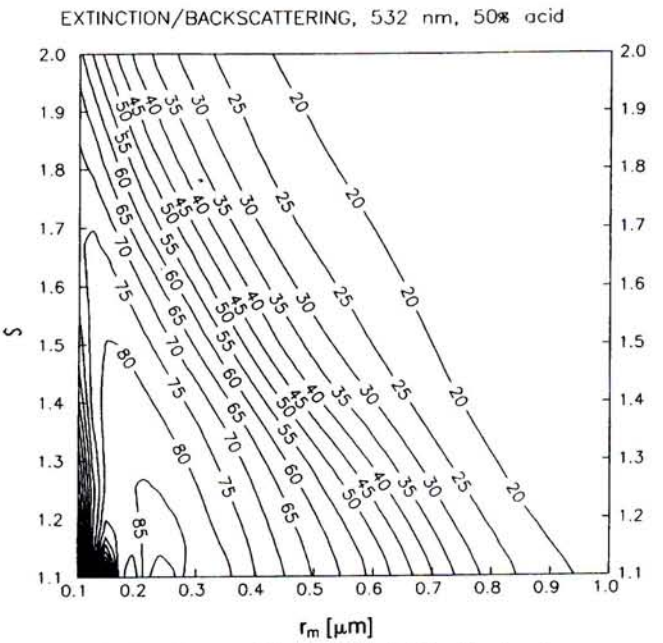

Fig. 3. Same as Fig. 2 but for 50% sulfuric acid.

of k_j, as computed for a monomodal size distribution characterized by r_m and s.

The minima of χ^2 provide a set of optimal (r_m, s) pairs.

Only the data at the 355-, 532-, and 750-nm wavelengths have been considered reliable for this purpose, because of the large statistical dispersion of the 850-nm data.

Monomodal log-normal distributions show quite good separation of the relative χ^2 minima, the deepest minima yielding stable size distributions. An example of χ^2 (r_m, s) surface for $Ro_{532} = 1.03$ and 50% sulfuric acid is shown in Fig. 11. Figure 11 shows

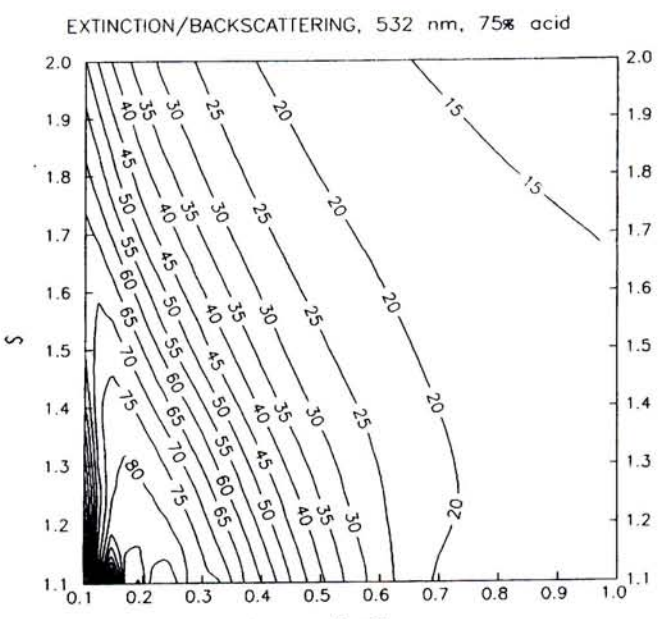

Fig. 4. Same as Fig. 2 but for 75% sulfuric acid.

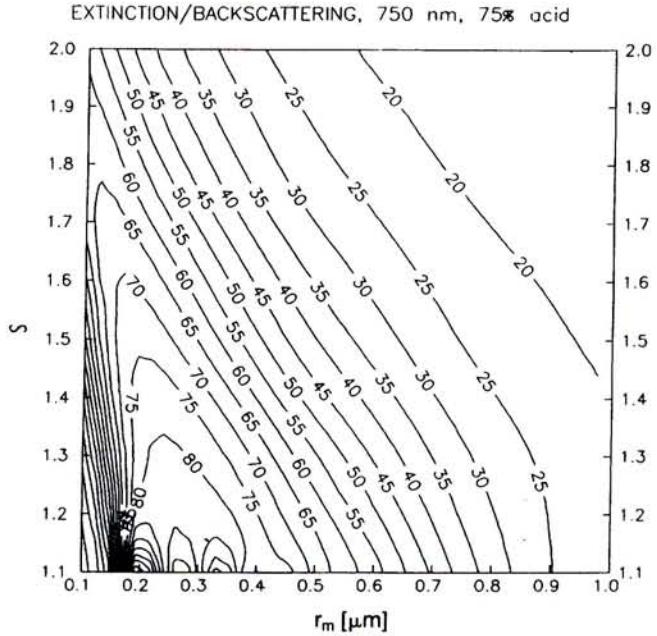

Fig. 5. Extinction/backscattering ratio at 750 nm (k_{750}) simulated for monomodal log-normal distributions of sulfuric acid droplets. The x axis is the mode radius r_m, and the y axis is the distribution dimensionless width s.

that the possible errors on r_m and s are strongly correlated because of the linear shape of the bottom of the χ^2 surface: an error of $+0.1$ μm on the retrieved r_m leads to an error of approximately -0.2 on s. This consideration is also valid for the other refractive indices used.

Resulting particle distributions for two refractive indices and three Ro hypothesis are reported in Table 2. Both 50% and 75% sulfuric acid have been considered, according to the expected range of concentrations at Mt. Pinatubo cloud heights.

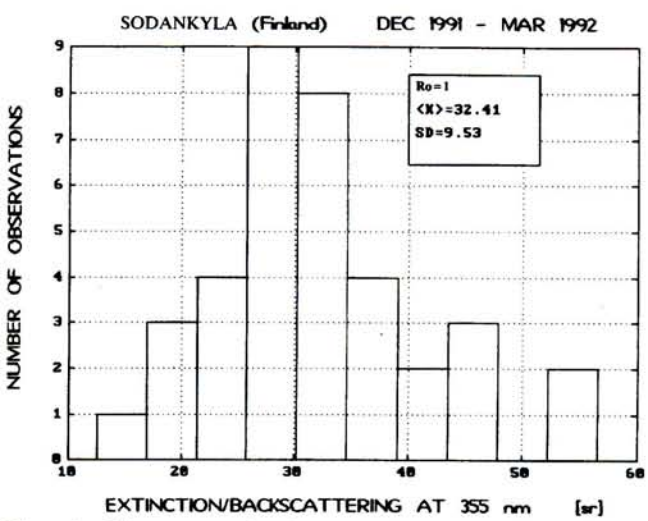

Fig. 6. Histogram of the experimental value of the extinction/backscattering ratio at 355 nm obtained under the hypothesis of molecular atmosphere ($R_o = 1$) below Mt. Pinatubo's aerosol layer.

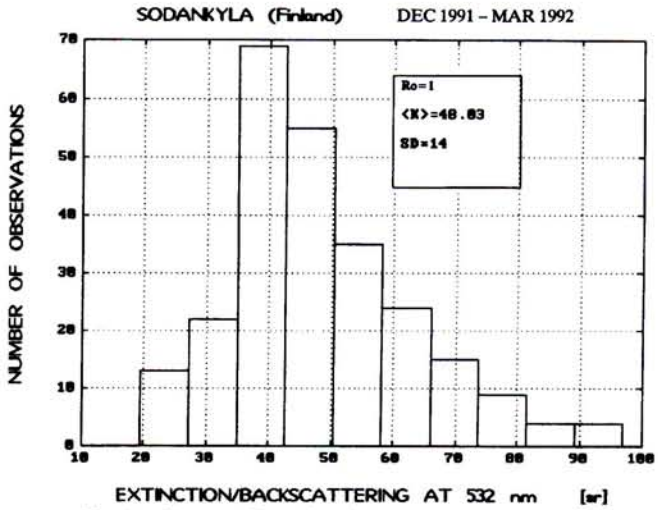

Fig. 7. Same as Fig. 6 but for 532-nm wavelength.

The sensitivity of optimal (r_m, s) pairs to the hypothesis concerning Ro_j is evident. The cases with $Ro_{532} = 1.03$–1.05 seem to be the most representative of the tropopause aerosol loading (as also suggested by the smaller values of χ^2), so that the corresponding (r_m, s) pairs should be more realistic than those obtained for $Ro_{532} = 1$. Finally, we note that 50% sulfuric acid yields smaller χ^2 values than does 75% sulfuric acid. This could reflect the real mean composition of the Mt. Pinatubo aerosols during the EASOE campaign. In fact the temperature in the main part of the Mt. Pinatubo aerosol layer ranged between approximately -65 °C and -75 °C above Sodankyla. With a stratospheric water concentration of 5 parts in 10^6, this range implies an aerosol sulfuric acid concentration between 40% and 70% at the equilibrium.

These results are fully comparable with those obtained by Larsen[14] with *in situ* measurements performed by means of balloon-borne backscatter sondes, with our results showing similar r_m values but a wider distribution ($s \approx 1.8$–2 against $s \approx 1.3$–1.7). The size distributions retrieved by our method

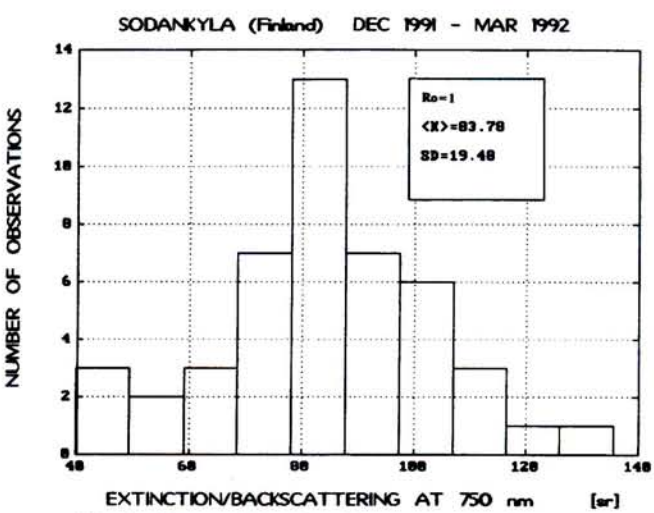

Fig. 8. Same as Fig. 6 but for 750-nm wavelength.

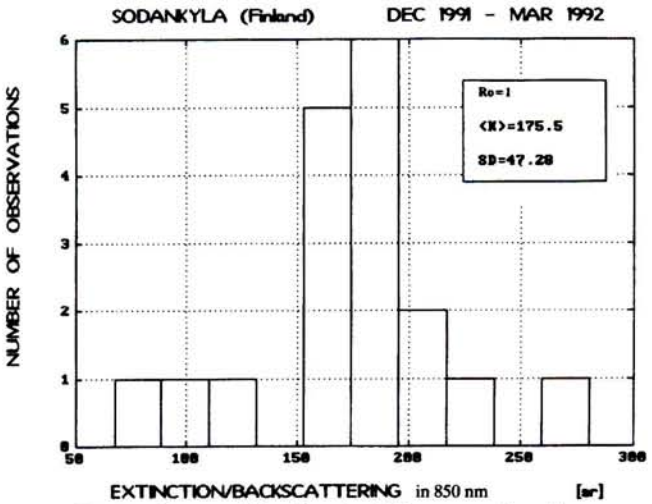

Fig. 9. Same as Fig. 6 but for 850-nm wavelength.

are partially in agreement with those detected by Deshler *et al.*[15] by means of dust sondes in Wyoming, a few months after the Mt. Pinatubo eruption. In such a case the following distributions for fresh aerosols were observed: ($r_m = 0.075$, $s = 1.9$) in the lower part of Mt. Pinatubo cloud and ($r_m = 0.35$, $s = 1.6$) in the higher part of the cloud.

Our results match better with the dust sonde measurements carried out by Deshler[16] in Kiruna, Sweden, during the EASOE campaign, from which Deshler estimated monomodal distributions with $r_m \approx 0.09$–0.14 μm and with rather wide distributions ($s \approx 1.9$–2). Our results are also in substantial agreement with the results obtained by Kolenda *et al.*[5]

6. Attempt to Derive a Bimodal Size Distribution

The sum of two log normals has been used to simulate a bimodal distribution of stratospheric aerosols, as suggested by Hofmann *et al.*[11] The first log normal reproduces a bulk aerosol distribution, corresponding to the background aerosols enhanced by the volcanic eruption, composed of sulfuric acid with small mode

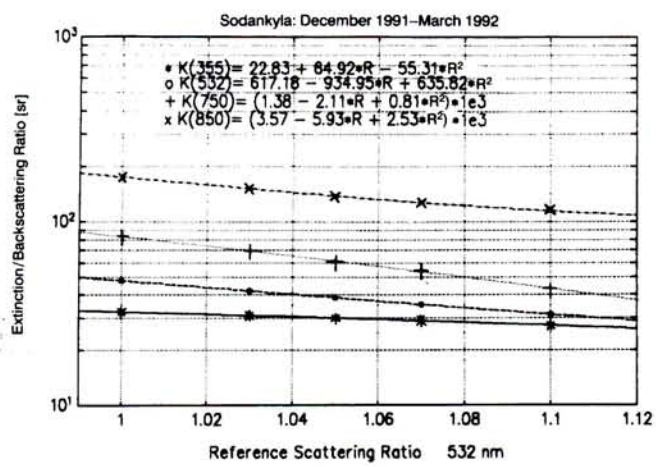

Fig. 10. Dependency of k_j from the value R_{532} assumed below the Mt. Pinatubo aerosol layer. The linear fits of the results are reported. k_j units are [sr].

Table 1. Experimental Extinction/Backscattering Ratios (k_j) and Relative Standard Deviations (σ_j) at the Different Laser Wavelengths and with Three Hypotheses on *Ro* Below the Cloud Base

Reference Scattering Ratio	Wavelength (nm) 355	532	750	850
$Ro_{532} = 1$				
k_j (sr)	32.4	48	84	175
σ_j (sr)	9.5	14.6	20	47
$Ro_{532} = 1.03$				
k_j (sr)	31	42	70	153
σ_j (sr)	10	14.7	20	48
$Ro_{532} = 1.05$				
k_j (sr)	30	39	61.4	139.5
σ_j (sr)	10	15	20	49

radius r_b, width distribution s_b, total number N, and variable refractive index; the second log normal simulates the coarse volcanic aerosols, with mode radius r_m, width s, density ratio N_b/N with respect to the bulk aerosols, and variable refractive index.

All these seven parameters should be varied in Mie simulations to obtain a bimodal distribution, whereas using all four values of k_j data, we can retrieve a maximum of four parameters. To reduce the amount of the variable quantities involved, we have assumed the refractive index of the bulk aerosols to be constant (the refractive index of 75% liquid sulfuric acid has been imposed), and two other quantities (r_b and the coarse particles' refractive index) have been considered as parameters. Under such bounds, minima of χ^2 can potentially give a set of minimal distributions.

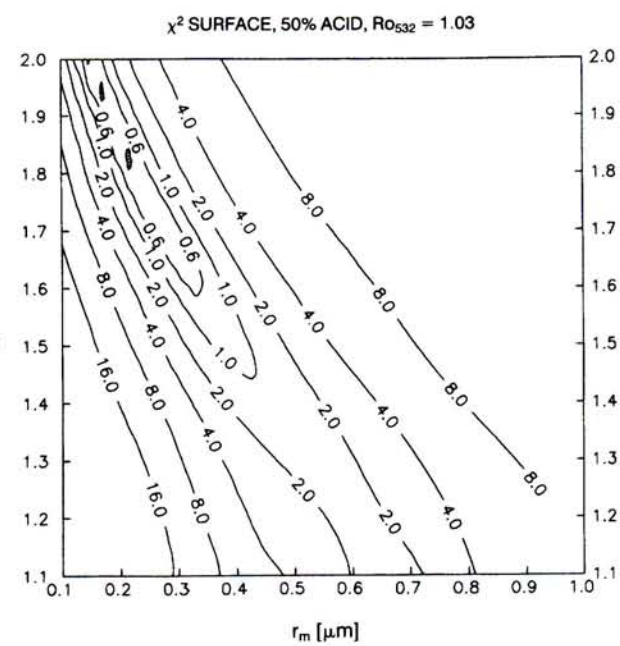

Fig. 11. Constant-value plot of $\chi^2(r_m, s)$ for a monomodal distribution. The hatched areas are the bottom of the χ^2 surface, corresponding to the best fit of experimental k_j data with simulated k_j data for 50% sulfuric acid, $Ro_{532} = 1.03$.

Table 2. Retrieved Size Distributions (r_m, Mode Radius; s, Width) from 355-, 532-, and 750-nm Lidar Data under Three Hypothesis on Ro[a]

Composition (% sulfuric acid)	r_m (μm)	s	χ^2
Single log-normal fit ($Ro_j = 1$)			
50	0.27	1.65	0.59
75	0.22	1.55	0.90
Single log-normal fit ($Ro_{532} = 1.03$)			
50	0.22	1.8	0.26
75	0.18	1.75	0.49
Single log-normal fit ($Ro_{532} = 1.05$)			
50	0.18	2	0.2
75	0.13	2	0.32

[a]The hypothesis that $Ro_{532} = 1.03$–1.05 seems to be more reasonable than $Ro = 1$ in the upper troposphere.

For a good separation of χ^2 minima a similar precision for all four values of k_j is required, but in our case k_{750} and (particularly) k_{850} show wide data dispersion. The relative weight of k_{850} in the χ^2 analysis is then small, and our case practically corresponds to the case of three wavelengths, the distances between different minima being reduced.

Further considerations are necessary. As a consequence of the characteristic hill-shaped k_j constant-value plots (e.g., Fig. 2) and because of the independence of k_j from aerosol number density, the ratio N_b/N is much more uncertain than r_m, s, and s_b. In fact for each observed $\{k_j\}$ set, two distinct χ^2 minima can exist for monomodal distributions, one on the left slope of the k_j hill, the other on the right side. In our case the first minimum corresponds to a monomodal log-normal distribution of particles with r_m of the order of 0.1 μm (bulk aerosols), and the second minimum corresponds to a distribution of coarse particles with r_m of approximately 0.2–0.6 μm.

If such two minima make similar individual contributions to χ^2, then when bimodal distributions are used the N_b/N ratio remains unknown because of the degeneration of χ^2 solutions. All these problems are due to the particular nonlinearity of the system of $k_j = f_j(r_m, s, s_b, N_b/N)$ functions to be solved by means of the χ^2 method, because the solutions also degenerate when there are as many unknown variables as there are known terms k_j.

For all these reasons the computed values of N_b/N are particularly unreliable. They should be considered merely as a rough estimation. In spite of such uncertainties, the deepest minima of χ^2 can still provide some information concerning the size distributions and the dispersion of the retrieved parameters. The range of the distribution parameters corresponding to the five deepest minima for each acid concentration of the bulk aerosols and the different Ro_{532} are listed in Tables 3 and 4, for both $Ro_{532} = 1$ and $Ro_{532} = 1.05$.

Table 3. Bimodal Distribution Fitting of Lidar Data[a]

CAC[b]	r_b (μm)	s_b	r_m (μm)	s	N_b/N
50%	0.05	1.5–1.9	0.3–0.4	1.5–1.6	40/60
	0.1	1.7–1.8	0.5–0.6	1.3–1.4	20/50
	0.15	1.5–1.6	0.5–0.6	1.3–1.4	10/20
75%	0.05	1.5–1.9	0.3–0.5	1.1–1.4	50/60
	0.1	1.8–1.9	0.55	1.1	50/60
	0.15	1.8–1.9	0.5–0.55	1.1	30/60

[a]$Ro = 1$, 75% acid bulk aerosols.
[b]Coarse aerosol sulfuric acid concentration.

Table 4. Bimodal Distribution Fitting of Lidar Data[a]

CAC[b]	r_b (μm)	s_b	r_m (μm)	s	N_b/N[c]
50%	0.05	1.8–1.9	0.5–0.6	1.3–1.4	50–60
	0.1	1.5–1.8	0.6	1.3–1.4	20–30
	0.15	1.5–1.7	0.55–0.6	1.4	10–20
75%	0.05	1.6–1.9	0.35–0.5	1.2–1.4	60
	0.1	1.7–1.9	0.55–0.6	1.1	30–60
	0.15	1.6–1.8	0.55–0.6	1.1	20–30

[a]$Ro_{532} = 1.05$, 75% acid bulk aerosols.
[b]Coarse aerosol sulfuric acid concentration.
[c]Ratio between bulk and coarse aerosol total numbers.

The values computed for r_m, s_b, and s are fully comparable with those obtained by Deshler *et al.*[15] in Wyoming, some months after the eruption of Mt. Pinatubo, and by Deshler[16] in Kiruna during EASOE campaign by means of particle counters, particularly for the case with $Ro_{532} = 1.05$, 75% sulfuric acid, and $r_b = 0.05$–0.1 μm.

If the independence of k_j on the aerosol concentration is an advantage of the method used (allowing us to use the value of k_j obtained as the average over different lidar profiles), for the same reason the absolute number density cannot be retrieved directly. Evaluating the aerosol number density from the retrieved distribution parameters requires that we first compute the Mie backscattering coefficient at one wavelength for a single particle (β_1). The total number Nt (or N_b and N for bimodal distributions) can be obtained as the ratio between local Mt. Pinatubo backscattering $\beta(z)$ and β_1.

7. Conclusions

The use of lidar-derived multiwavelength extinction/backscattering ratios was found to be a promising method for the remote measurement of the size distribution of stratospheric aerosols. The main uncertainties involved in such a method are due to incomplete knowledge of the particle refractive index and of the actual aerosol loading below the base of the aerosol layer. The method gives meaningful results with monomodal fitting distributions when particle size is almost uniform within the cloud, because only a height-averaged size distribution shape is obtained with the method. The size distribution shape should also be slowly varying with time, an averaging of k_j values coming from many different lidar profiles (taken at different times) being necessary to obtain reliable mean values. k_j are in fact affected by large errors resulting from the natural fluctuations of Ro_j at the cloud base.

The aged stratospheric volcanic aerosols measured during the EASOE campaign seem to verify all these hypothesis, as suggested by the agreement of our results with other *in situ* optical measurements of particle size carried out before and during the EASOE.

The suggested method could in principle be used in long-term monitoring of the mean stratospheric aerosol monomodal size distribution for climate modeling purposes. A successful fitting of the lidar data by means of bimodal log-normal distributions is reported in this paper. Such fitting requires the introduction of several arbitrary hypotheses about the nature of the aerosols and does not allow us to determine the aerosol total numbers corresponding to the two modes because of the particular nonlinear scattering properties of the sulfuric aerosols in the investigated size range.

We thank the Sodankyla Finnish Meteorological Institute station staff; F. Castagnoli, V. M. Sacco, V. Venturi, and L. Zuccagnoli of the Istituto di Ricerca sulle Onde Elletromagnetiche; J. Kolenda and P. Rairoux of Freie Universität; and R. Matthey of the Observatoire Cantonal de Neuchâtel. We thank the European Community for its financial support of the EASOE campaign.

References

1. L. Stefanutti, F. Castagnoli, M. Del Guasta, M. Morandi, V. M. Sacco, V. Venturi, L. Zuccagnoli, J. Kolenda, H. Kneipp, P. Rairoux, B. Stein, D. Weidauer, and J. P. Wolf, "A four wavelength depolarization backscattering lidar for PSC monitoring," Appl. Phys. **55,** 13–17 (1992).
2. J. D. Klett, "Stable analytical inversion solution for processing lidar returns," Appl. Opt. **20,** 211–220 (1981).
3. J. D. Klett, "Lidar inversion with variable backscattering/extinction ratio," Appl. Opt. **24,** 1638–1643 (1985).
4. M. Morandi, "A complete procedure for inverting backscattering lidar returns," Research Rep. RR/GCF/92.11 (Istituto di Ricerca sulle Onde Elletromagnetiche, Firenzo, Italy, 1992).
5. J. Kolenda, B. Mielke, P. Rairoux, B. Stein, M. Del Guasta, D. Weidauer, J. P. Wolf, L. Woste, F. Castagnoli, M. Del Guasta, M. Morandi, V. M. Sacco, L. Stefanutti, V. Venturi, and L. Zuccagnoli, "Aerosol size distribution measurements using a multispectral lidar-system," in *Lidar for Remote Sensing,* R. J. Becherer, R. M. Hardesty, and J. P. Meyzonnette, eds., Proc. Soc. Photo-Opt. Instrum. Eng. **1714,** 209–219 (1992).
6. K. Parmameswaran, K. O. Rose, and B. V. Krishna Murty, "Relationship between backscattering and extinction coefficients of aerosols with application to turbid atmosphere," Appl. Opt. **30,** 3059–3071 (1991).
7. H. C. van de Hulst, *Light Scattering by Small Particles* (Wiley, New York, 1957), Chap. 9, pp. 114–128.
8. M. Del Guasta, "A FORTRAN code for quick computing of light scattered by spherical particles, with particular reference to backscattering lidar," CNR Rep. TR/GCF/91.22 (Istituto di Ricerca sulle Onde Elletromagnetiche, Firenze, Italy, 1992).
9. K. F. Palmer and D. Williams, "Optical constants of sulfuric acid: application to the clouds of Venus," Appl. Opt. **14,** 208–219 (1975).
10. S. G. Warren, "Optical constants of ice from the ultraviolet to the microwave," Appl. Opt. **23,** 1206–1225 (1984).
11. D. J. Hofmann, J. M. Rosen, R. Reiter, and H. Jager, "Lidar and balloonborne particle counter comparison following recent volcanic eruptions," J. Geophys. Res. **88,** 3777–3782 (1983).
12. C. Brogniez and J. Lenoble, "Analysis of the 5-year aerosol data from stratospheric aerosol and gas experiment II," J. Geophys. Res. **96,** 15479–15497 (1991).
13. M. Morandi, "EASOE four wavelength lidar data analysis: preliminary reuslts," Tech. Rep. TR/GCF/92.27 (Istituto di Ricerca sulle Onde Elletromagnetiche, Firenze, Italy, 1992).
14. N. Larsen, "Stratospheric aerosols: backscatter measurements from Thule European Arctic Stratospheric Ozone Experiment," Danish Meteorological Institute Scientific Rep. 92-1 (Danish Meteorological Institute, Copenhagen, 1992).
15. T. Deshler, D. J. Hofmann, B. J. Johnson, and W. R. Rozier, "Balloonborne measurements of the Pinatubo aerosol size distribution and volatility at Laramie, Wyoming during the summer of 1991," Geophys. Res. Lett. **8,** 21–22 (1992).
16. T. Deshler, "In situ measurements of the size distribution of the Pinatubo aerosol over Kiruna on four days between 18 January and 13 February 1992," submitted to Geophys. Res. Lett.